A stochastic-deterministic coupling method for multiscale problems. Application to numerical homogenization of random materials

Régis Cottereau

Available online at www.sciencedirect.com

SciVerse ScienceDirect

Procedia IUTAM 00 (2012) 000-000

Procedia IUTAM

www.elsevier.com/locate/procedia

IUTAM Symposium on Multiscale Problems in Stochastic Mechanics 2012

A stochastic-deterministic coupling method for multiscale problems. Application to numerical homogenization of random materials

Régis Cottereau[a]

[a]*Laboratoire MSSMat UMR 8579, École Centrale Paris, CNRS, F-92295 Châtenay-Malabry, France*

Abstract

In this paper, we describe a multiscale strategy that allows to couple stochastic and deterministic models. The transition condition enforced between the two models is weak, in the sense that it is based on volume coupling in space (rather than more classical boundary coupling) and on a volume/sample average in the random dimension. The paper then concentrates on the application of this weak coupling technique for the development of a new iterative method for the homogenization of random media. The technique is based on the coupling of the stochastic microstructure to a tentative homogenized medium, the parameters of which are initially chosen at will. Based on the results of the coupled simulation, for which Dirichlet or Neumann boundary conditions are posed at the boundary of the tentative homogenized medium, the parameters of the homogenized medium are then iteratively updated. An example shows the efficiency of the proposed approach compared to the classical KUBC and SUBC approaches in stochastic homogenization.Selection and/or peer-review under responsibility of Karlsruhe Institute of Technology (KIT), Institute of the Engineering Mechanics.

Keywords: Homogenization; Random material; Arlequin method; self-consistent model; Numerical mesoscope

1. Introduction

Classical deterministic models provide global predictions that are satisfactory for many industrial applications. However, when one is interested in a very localized behavior or quantity, or when multiscale phenomena come into play, these models may not be sufficient. For instance, the limited heterogeneity of a material modeled as a continuum might have no influence on its behavior on a large scale, while the study of a local stress intensity factor would strongly depend on the local heterogeneity of the mechanical parameters. Unfortunately, for these problems, the information necessary to parameterize the relevant, very complex, models is usually not available. Stochastic methods have therefore been proposed and now appear unavoidable in multiscale modeling. Although the use of stochastic models and methods has expanded rapidly in the last decades, the related numerical costs are still often prohibitive. Hence, the application of these methods in a complex or industrial context remains limited. An important field of research is therefore concerned with the reduction of the costs associated with the use of stochastic methods, for example by using

* Corresponding author. Tel.: +33-(0)1 41 13 13 56 ; fax: +33 (0)1 41 13 14 42 .
E-mail address: regis.cottereau@ecp.fr

iterative methods specially adapted to the structure of the matrices arising in the Stochastic Finite Element method, using reduced bases for the representation of random fields, or using special domain decomposition techniques for parallel resolution on clusters of computers.

The first part of this paper describes an alternative to these purely mathematical/numerical approaches through the coupling of two models: one deterministic and one stochastic. The general goal is that of modeling a global problem in a mean or homogeneous way where it yields sufficient accuracy, while retaining a stochastic model where needed. Hence, additional complexity is added in the model only where required, and the general approach is both more elegant and numerically cheaper than a global all-over stochastic model would be. Further, the cuts on computational costs mean that industrial applications come within reach. The core idea is to extend the Arlequin coupling method, described in a general setting in [1, 2], to the case of the coupling of a stochastic model with a deterministic one. The main ingredients are the choices of the operator and functional space for the coupling, and are described in detail in [3, 4]. They will be recalled and summarized in this first part of the paper. The most interesting feature of the coupling strategy is that it really couples the random microstructure with the deterministic homogenized model, and not one (deterministic) realization of the random medium with a homogenized model.

For the first part of this paper, it is assumed that both the stochastic microstructure model and the corresponding deterministic macroscale model are available. However, in practice, it is often a difficult task to derive the homogenized model corresponding to a given stochastic microstructure. This question has been treated extensively in the mathematical literature, starting with [5, 6, 7, 8] and many existence results have been obtained for different random media [9, 10, 11, 12, 13]. Fewer results, however, exist for the computation of homogenized models corresponding to actual microstructures [9, 14, 15]. The basic problem lies in the requirement to cut the physical space at finite length (no periodicity hypothesis *a priori*) for computational reasons, hence introducing a bias in the estimate of the homogenized coefficients. We propose in the second part of this paper a new numerical homogenization strategy that attempts to solve that issue. It is based on the previous stochastic-deterministic coupling approach, and on a self-consistent iterative process to update the value of the homogenized tensor until convergence. The general idea of the scheme is exactly the same as that of self-consistent homogenization, although it is here performed numerically and extended to stochastic homogenization. Through the volume coupling, the boundary conditions (in space and random dimension) are repulsed away from the stochastic microstructure, and the ergodicity of the random medium can be used in full to accelerate convergence. The weakness of the coupling, both in the space and the stochastic dimensions, is essential in order not to create a strong properties contrast between the two models, as in [16].

Throughout the paper, we will use bold characters for random quantities, lowercase characters for scalars and vectors, and uppercase characters for matrices and tensors.

2. A stochastic-deterministic coupling method

Let us consider a (stochastic) microstructure defined over a domain D, with a stochastic parameter field $\boldsymbol{k}(x)$, and a (deterministic) effective model defined over a domain $\underline{D}$, with a constant parameter $\underline{K}$. The supports of the two models are such that $D \subset \underline{D}$, and we also define a subset of their intersection $D_c \subset \underline{D}$, over which they will be considered to communicate. These definitions mean that there is part of the domain where only the effective model is defined, part of the domain where both models are defined and over which they are coupled, and part of the domain where both models are defined but over which they do not communicate.

The coupling problem is set in the general Arlequin framework (see in particular [1, 17, 2, 18] for details on the Arlequin framework in a deterministic setting and [3, 4] for the stochastic case), and is recalled here in the particular context of the homogenization technique that will be presented in the next section. It reads: find $(\underline{u}, \boldsymbol{u}, \boldsymbol{\Phi}) \in \underline{\mathscr{V}} \times \mathscr{W} \times \mathscr{W}_c$ such that

$$\begin{cases} a(\underline{u}, v) + C(\boldsymbol{\Phi}, v) = \ell(v), & \forall v \in \underline{\mathscr{V}} \\ \mathscr{A}(\boldsymbol{u}, \boldsymbol{v}) - C(\boldsymbol{\Phi}, \boldsymbol{v}) = 0, & \forall \boldsymbol{v} \in \mathscr{W} \\ C(\boldsymbol{\Psi}, \underline{u} - \boldsymbol{u}) = 0, & \forall \boldsymbol{\Psi} \in \mathscr{W}_c \end{cases}, \tag{1}$$

where the forms a and $\mathscr{A}$ are the forms corresponding to the equations driving the two models, weighted by two weight functions α_1 and α_2 that enforce the conservation of the global energy, by appropriate partitioning among the

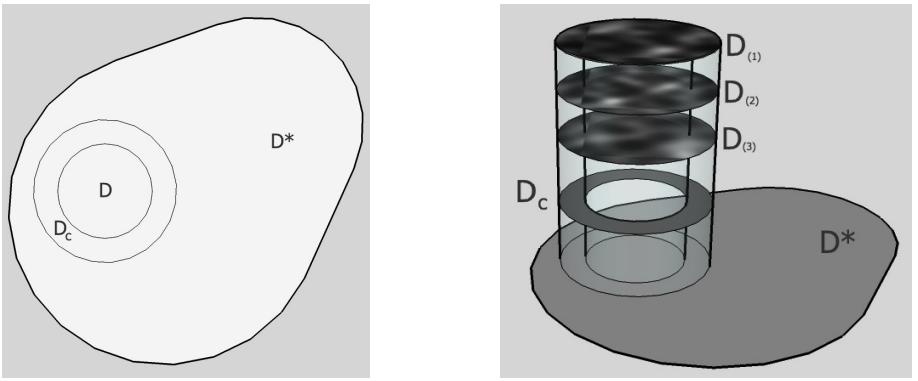

Fig. 1. Section (left) and perspective view (right) of a 2D Arlequin problem where an effective model, defined over domain $\underline{D}$, and several realizations of a random model, defined over D, are coupled through a coupling domain D_c. On the overlap outside of D_c: $(D \cap \underline{D}) \backslash D_c$, both models are defined but behave independently.

two available models. More specifically, these forms are:

$$a(u,v) = \int_{\underline{D}} \alpha_1(x) \underline{K} \nabla u \cdot \nabla v \, dx, \tag{2}$$

and

$$\mathscr{A}(\boldsymbol{u},\boldsymbol{v}) = \mathrm{E}\left[\int_D \alpha_2(x) \boldsymbol{k}(x) \, \nabla \boldsymbol{u} \cdot \nabla \boldsymbol{v} \, dx \right]. \tag{3}$$

The weight functions allow to put emphasis on one or the other of the two models. Hence, where the stochastic (fine scale) model is defined (and outside of the coupling area), the weight function $\alpha_2(x)$ is given a value close to one (and $\alpha_1(x)$ a value close to zero). We will consider in this paper surface loading at the boundary of the deterministic model: $\ell(v) = \int_{\partial \underline{D}} g_0 v dx$, with typically $g_0 = 1$ (for Neumann approach, see further) or $g_0 = 0$ (for Dirichlet approach).

The coupling operator C enforces weakly the equality of the two fields $\boldsymbol{u}$ and $\underline{u}$ in the coupling area D_c. It is defined by:

$$C(\boldsymbol{u},\boldsymbol{v}) = \mathrm{E}\left[\int_{D_c} (\kappa_0 \boldsymbol{u}\boldsymbol{v} + \kappa_1 \nabla \boldsymbol{u} \cdot \nabla \boldsymbol{v}) \, dx \right], \tag{4}$$

with κ_0 and κ_1 two constant given parameters. Concerning the choice of functional spaces, we will consider in this paper $\underline{\mathscr{V}} = \mathscr{H}^1_x(\underline{D})$ for homogeneous unit Dirichlet boundary conditions around $\underline{D}$, and $\underline{\mathscr{V}} = \mathscr{H}^1_0(\underline{D})$ for homogeneous unit Neumann boundary conditions. The other spaces are $\mathscr{W} = \mathscr{L}^2(\Theta, \mathscr{H}^1(D))$ and

$$\begin{aligned} \mathscr{W}_c &= \mathscr{H}^1(D_c) \oplus \mathscr{L}^2(\Theta, \mathbb{R}) & (5) \\ &= \left\{ \psi(x) + \boldsymbol{\theta} \mathbb{I}_c(x) | \psi \in \mathscr{H}^1(D_c), \boldsymbol{\theta} \in \mathscr{L}^2(\Theta, \mathbb{R}) \right\}. & (6) \end{aligned}$$

The indicator function $\mathbb{I}_c(x)$ is such that $\mathbb{I}_c(x \in D_c) = 1$ and $\mathbb{I}_c(x \notin D_c) = 0$. Hence the mediator space $\mathscr{W}_c$ can be seen as composed of functions with a spatially varying mean and perfectly spatially correlated randomness. Thanks to the specific structure of the space $\mathscr{W}_c$, the last equality of the system (1) can be written equivalently, $\forall \boldsymbol{\Psi} = \psi(x) + \boldsymbol{\theta} \mathbb{I}_c(x) \in \mathscr{W}_c$, or otherwise said, $\forall \psi \in \mathscr{H}^1(D_c)$ and $\forall \boldsymbol{\theta} \in \mathscr{L}^2(\Theta, \mathbb{R})$,

$$\begin{aligned} 0 &= C(\boldsymbol{\Psi}, \underline{u}_\varepsilon - \boldsymbol{u}_\varepsilon) & (7) \\ &= \mathrm{E}\left[\int_{\Omega_c} (\kappa_0 (\psi + \boldsymbol{\theta} \mathbb{I}_c)(\underline{u}_\varepsilon - \boldsymbol{u}_\varepsilon) + \kappa_1 \nabla \psi \cdot \nabla (\underline{u}_\varepsilon - \boldsymbol{u}_\varepsilon)) \, dx \right] & (8) \\ &= C(\mathrm{E}[\boldsymbol{\Psi}], \underline{u}_\varepsilon - \mathrm{E}[\boldsymbol{u}_\varepsilon]) - \mathrm{E}\left[\boldsymbol{\theta} \int_{\Omega_c} (\boldsymbol{u}_\varepsilon - \mathrm{E}[\boldsymbol{u}_\varepsilon]) \, dx \right]. & (9) \end{aligned}$$

Therefore, this condition imposes that, in each space point $x \in D_c$, the (ensemble) average of the random field $\mathrm{E}[\boldsymbol{u}_\varepsilon(x)]$ should be equal to the field $\underline{u}_\varepsilon(x)$, and that the variability of the space-averaged random variable $\int_{\Omega_c} (\boldsymbol{u}_\varepsilon - \mathrm{E}[\boldsymbol{u}_\varepsilon])dx$ should cancel. It should be noted that this condition is the weakest possible in order to maintain solvability of the coupled system. The stability of the coupled problem (1) was proved in [4], and its solution can be provided either by Monte Carlo sampling of the random space, or by a spectral approach.

3. A new method for the numerical homogenization of random materials

Before presenting the numerical homogenization technique we propose to introduce, we recall some definitions of homogenization of random media.

3.1. Definition of homogenization

Let us introduce a domain $D \in \mathbb{R}^d$, with a typical length scale L, a (deterministic) loading field $f(x)$ and a field $\boldsymbol{u}(x)$ verifying the random heat equation: find $\boldsymbol{u}(x) \in \mathscr{L}^2(\Theta, \mathscr{L}^2(D))$ such that, $\forall x \in D$, almost surely:

$$-\nabla \cdot (\boldsymbol{k}(x) \nabla \boldsymbol{u}(x)) = f(x), \tag{10}$$

for a random field $\boldsymbol{k}(x)$ fluctuating over a length scale ℓ_c (usually defined through the correlation length), and with appropriate boundary conditions. Here, $(\Theta, \mathscr{F}, P)$ is a complete probability space, with Θ a set of outcomes, $\mathscr{F}$ a σ-algebra of events of Θ, and $P : \mathscr{F} \to [0,1]$ a probability measure.

Homogenization deals with the situation when the ratio $\varepsilon = \ell_c / L$ is small. We then scale the fluctuations of the microstructure by $1/\varepsilon$, and look at the fluctuations of the solution $\boldsymbol{u}(x)$ at the original scale. The following sequence of problems is therefore considered: find $\boldsymbol{u}_\varepsilon(x) \in \mathscr{L}^2(\Theta, \mathscr{L}^2(D))$ such that, $\forall x \in D$, almost surely:

$$-\nabla \cdot (\boldsymbol{k}_\varepsilon(x) \nabla \boldsymbol{u}_\varepsilon(x)) = f(x), \tag{11}$$

where $\boldsymbol{k}_\varepsilon(x) = \boldsymbol{k}(x/\varepsilon)$, and with appropriate boundary conditions (for instance $\boldsymbol{u}_\varepsilon(x) = 0$ and $\forall x \in \partial D$ for the definition of Dirichlet and Neumann approximations of the homogenized coefficients). Under suitable hypotheses, in particular on the random field $\boldsymbol{k}_\varepsilon(x)$, each of these problems admits a unique solution.

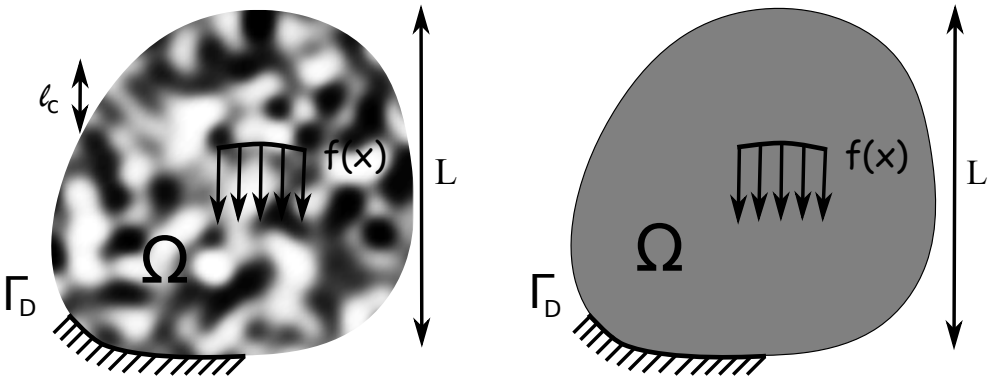

Fig. 2. Description of one realization of the random medium (left), with fluctuating coefficient $\boldsymbol{k}_\varepsilon(x)$, and corresponding effective medium (right), with constant deterministic effective tensor K^*.

Using different sets of hypotheses and with different methods, many authors (see the bibliography in the introduction) have shown that, independently of the load $f(x)$, the sequence of solutions $\boldsymbol{u}_\varepsilon(x)$ converges when $\varepsilon \to 0$ to the solution $u^*(x)$ of the following deterministic problem: find $u^*(x) \in \mathscr{L}^2(D)$ such that, $\forall x \in D$:

$$-\nabla \cdot (K^* \nabla u^*(x)) = f(x), \tag{12}$$

with corresponding boundary conditions. *A priori*, the effective coefficient K^* is a full second-order tensor, meaning that the homogenized material potentially exhibits anisotropy.

The constructive definition of the effective tensor requires the solution of the so-called corrector problems, which state: find $\boldsymbol{w}_\varepsilon(x) \in \mathscr{L}^2(\Theta, (\mathscr{L}^2(D))^d)$ such that, $\forall x \in D$, almost surely:

$$-\nabla \cdot (\boldsymbol{k}_\varepsilon(x)\,(I + \nabla \boldsymbol{w}_\varepsilon(x))) = 0. \tag{13}$$

As $\boldsymbol{w}_\varepsilon$ is a vector, $\nabla \boldsymbol{w}_\varepsilon(x)$ is a tensor, and this equation is a d-dimensional equation. The tensor I is the identity tensor in $\mathbb{R}^d \times \mathbb{R}^d$. The homogenized tensor is then defined as:

$$K^* = \lim_{\varepsilon \to 0} \mathrm{E}\left[(I + \nabla \boldsymbol{w}_\varepsilon(x))^T \boldsymbol{k}_\varepsilon(x)\,(I + \nabla \boldsymbol{w}_\varepsilon(x)) \right]. \tag{14}$$

Approximate values of the homogenized tensor can be estimated by considering finite values of the ratio ε, and imposing unit-strain boundary condition (hence obtaining the KUBC estimate) or unit-stress boundary conditions (hence obtaining the SUBC estimate). The estimates are biased and bound (SUBC from below, and KUBC from above) the exact homogenized coefficient. In the next section, we introduce an alternative approach for computing approximations of the homogenized coefficients, with less bias.

3.2. Principle of the method

The general motivation for the design of this technique lies in the observation that the biases observed in the SUBC and KUBC estimates of the homogenized coefficients originate from the boundary conditions chosen for each realization of the random corrector problems. Somehow, in order to obtain good estimates of the homogenized coefficients, these boundary conditions have to be taken away (by reducing ε), in order to minimize their influence. The approach that we propose here builds on this idea, originally proposed by [16]. However, it brings down the issues encountered by these authors by considering a volume coupling, which is much smoother than an interface-based one. Further, it allows to perform the coupling between the entire set of realizations of the random medium and the tentative homogenized medium through the coupling operator described in equation (4), which is extremely weak and hence introduces less stiffness mismatch.

The issue with that approach is that it is necessary to know beforehand the value of the homogenized coefficient in order to construct the coupled Arlequin model. We therefore construct the estimate of the homogenized tensor through a fixed-point iterative scheme. This optimization scheme builds on the idea that, once the homogenized model has been identified, it should behave exactly the same, whether it is solved alone or coupled to the micro-structure it represents. In particular, the solution of a coupled Arlequin problem with that homogenized model and the micro-structure under homogeneous Dirichlet or Neumann boundary conditions should yield exactly the same result as if the homogenized model was solved alone. On the other hand, if the tentative homogenized model is not correct, there will be a mismatch of impedances that can be detected through the distance between the response of the homogenized model in the coupled model and that of the same homogenized model solved alone.

Algorithm 1: Algorithmic description of the proposed iterative technique for numerical homogenization of random materials with Dirichlet boundary conditions

Data: N realizations of random medium $\boldsymbol{k}_\varepsilon(x)$ of correlation length ε
Result: Dirichlet Arlequin estimate of homogenized tensor $\underline{\check{K}}_N^\varepsilon$

Initialization: $K_0 \longleftarrow \mathrm{E}[\boldsymbol{k}_\varepsilon] I$;
while $\|K_i - K_{i-1}\| > \mathit{criterion}$ **do**
  set the mechanical parameter: $\underline{K}_\varepsilon \longleftarrow K_i$;
  solve the Arlequin coupled system (1) and estimate $(\underline{u}, \boldsymbol{u}, \boldsymbol{\Phi})$, with unit-strain boundary conditions at the boundary of $\underline{D}$;
  update K_{i+1} to minimize $\int_D \|\nabla \underline{u}_\varepsilon - I\| dx$
end
Store estimate: $\underline{\check{K}}_N^\varepsilon = K_i$.

3.3. Description of the algorithms

We present here two different algorithms: one for an estimate arising from imposing unit-strain boundary conditions around $\underline{D}$ (see algorithm 1), which corresponds to the classical KUBC estimate; and one for an estimate arising from imposing unit-stress boundary conditions around $\underline{D}$ (see algorithm 2), which corresponds to the classical SUBC estimate.

Algorithm 2: Algorithmic description of the proposed iterative technique for numerical homogenization of random materials with Neumann boundary conditions

Data: N realizations of random medium $\boldsymbol{k}_\varepsilon(x)$ of correlation length ε
Result: Neumann Arlequin estimate of homogenized tensor $\underline{\hat{K}}_N^\varepsilon$

Initialization: $K_0 \longleftarrow \mathrm{E}[\boldsymbol{k}_\varepsilon^{-1}]^{-1} I$;
while $\|K_i - K_{i-1}\| > criterion$ **do**
  set the mechanical parameter: $\underline{K} \longleftarrow K_i$;
  solve the Arlequin coupled system (1) and estimate $(\underline{u}, \boldsymbol{u}, \boldsymbol{\Phi})$, with unit-stress boundary conditions at the boundary of $\underline{D}$;
  update K_{i+1} to minimize $\int_D \|\underline{K}\nabla\underline{u} - I\| dx$
end
Store estimate: $\underline{\hat{K}}_N^\varepsilon = K_i$.

In these algorithms, note that the iterative loop can be efficiently implemented through classical general-purpose optimization schemes. In particular, we have used the Nelder-Mead algorithm (see [19] for details), but others could be considered. Similarly, we have chosen initial values for each of these algorithms that correspond to the arithmetic and harmonic averages, but other choices are equally reasonable.

4. Applications

In this section, we consider the implementation of our homogenization approach on a simple problem, for which an analytical solution is available. The software used for the solution of the coupled Arlequin systems is freely available at https://github.com/cottereau/CArl. In all the simulations presented in this section, we have used $\kappa_0 = 1$ and $\kappa_1 = 10^{-3}$ for the definition of the coupling operator (see Eq. (4)). Also, we have used $\alpha_2(x \in (\underline{D} \cap D) \backslash D_c) = 1 - \eta$ and $\alpha_1(x \in (\underline{D} \cap D) \backslash D_c) = \eta$, with $\eta = 10^{-3}$, for the weighting of the energies of the two models. The realizations of the random fields $\boldsymbol{k}_\varepsilon(x)$ have been generated using the spectral representation method [20], and its Fast Fourier Transform implementation. Finally, in the implementation of the loops in algorithm 1 and 2, a relative tolerance of $criterion = 10^{-2}$ was selected for both the value and the argument of the potential function .

We consider a two-dimensional problem, within a domain $D = [0,1] \times [0,1]$, of typical size $L = 1$. The operator to be homogenized is $\nabla \cdot \boldsymbol{k}_\varepsilon(x) \nabla \boldsymbol{u}_\varepsilon$, with $\boldsymbol{k}_\varepsilon(x)$ a random heterogeneous modulus. We consider for $\boldsymbol{k}_\varepsilon(x)$ a homogeneous random field with log-normal first-order marginal distribution, and average and standard deviation $\mathrm{E}[\boldsymbol{k}_\varepsilon] = \sigma = \sqrt{2}$. The power spectrum is considered triangular (which corresponds to a square cardinal sine correlation), with correlation length ℓ_c. We will consider the homogenization problem for three different relative correlation lengths: $\varepsilon = \ell_c / L = 10$, $\varepsilon = 1$ and $\varepsilon = 0.1$. These correlation lengths span several orders of magnitude (see figure 3 for examples of realizations of the random media considered) in order to show a wide range of behaviors for our method. Note that considering a domain of fixed size and variable correlation lengths, as is done here, is strictly equivalent to considering a constant random field homogenized over cells of variable sizes, as is more often done in the micro-mechanical community.

The homogenized tensor is known analytically [21] to be:

$$K^* = \begin{bmatrix} 1 & 0 \\ 0 & 1 \end{bmatrix}. \tag{15}$$

Indeed, the inverse of a log-normal random variable follows exactly the same law as the variable itself in the case when the mean and the standard deviation are equal. Note that, because we know beforehand that the homogenized

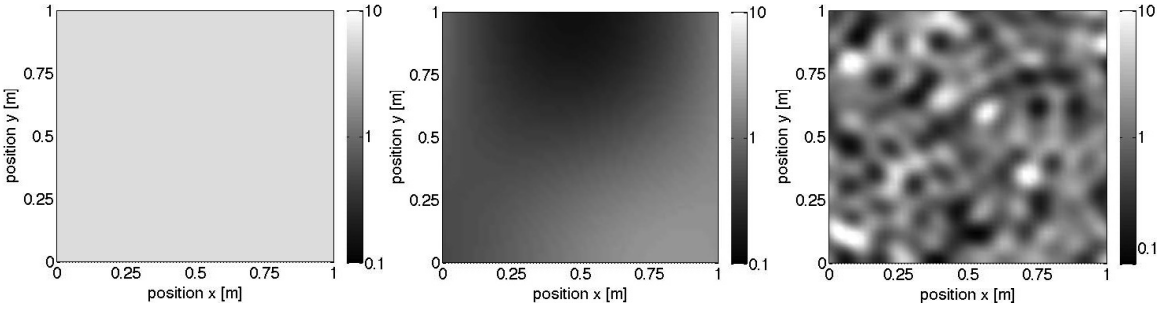

(a) $\varepsilon = 10$, Sample 1 (b) $\varepsilon = 1$, Sample 1 (c) $\varepsilon = 0.1$, Sample 1

Fig. 3. Map of parameter $\boldsymbol{k}_\varepsilon(x)$ (in logarithmic scale) for one realization of each of the cases considered here (left: $\varepsilon = \ell_c/L = 10$, center: $\varepsilon = 1$, and right: $\varepsilon = 0.1$).

tensor is isotropic, we will only discuss here the convergence toward the scalar value $K^*_{xx} = 1$. This means that the KUBC, SUBC, and Arlequin estimates will really be based only on numerical experiments in one direction (using only the imposed gradient $\nabla u_\varepsilon = [1\ 0]^T$ for the KUBC estimate for instance). More complex cases, with anisotropic homogenized behavior in particular, will be considered in the future.

First, we consider the KUBC and SUBC estimates of the homogenized coefficient. To observe the convergence with respect to the number N of realizations of the random medium over which averages are taken, we compute KUBC and SUBC estimates for different values of this number N. Note that, for a given correlation length, the values of the KUBC and SUBC estimates depend not only on the number N, but also on the realizations themselves. We therefore compute, for each value of N, $n = 10$ different estimates for different ensembles of N realizations of the random medium. These results are plotted in figure 4, as grey crosses for the KUBC and grey circles for the SUBC. The linear Finite Element method was used to compute the corrector problems, with 400, 800, and 5000 elements, respectively for the cases $\varepsilon = \ell_c/L = 10$, $\varepsilon = 1$ and $\varepsilon = 0.1$. On these plots, we retrieve the expected asymptotic behavior of the homogenized coefficients. Both the KUBC $\check{K}^\varepsilon_N$ and SUBC $\hat{K}^\varepsilon_N$ estimates converge to the exact value K^* for small ε and large N. Also, at large ε and large N, the KUBC estimate tends towards the arithmetic average $\mathrm{E}[\boldsymbol{k}_\varepsilon]$ and the SUBC estimate tends towards the harmonic average $\mathrm{E}[\boldsymbol{k}_\varepsilon^{-1}]^{-1}$.

We now turn to the estimation of the Arlequin estimate $\underline{K}^\varepsilon_N$ of the homogenized coefficient over domains $\underline{D} = [-1;2] \times [-1;2]$ and $D = [0;1] \times [0;1]$. The coupling zone D_c is a band of width 0.2 circling at the boundary of D, and we consider a unit strain boundary condition at the boundary of $\underline{D}$. This last condition means that we are really following the algorithm 1, and aim for Dirichlet Arlequin estimates $\underline{\check{K}}^\varepsilon_N$. In the Arlequin coupled problem (1), there exist the same typical lengths as before (ℓ_c and L), plus an additional one, corresponding to the size $\underline{L} = 3$ of the tentative homogeneous medium $\underline{D}$. In order to simplify the comparisons between the Arlequin estimate and the KUBC/SUBC estimates, we continue to define ε as the ratio of the correlation length ℓ_c to the size L of the random cell D, that actually indicates the amount of statistical information available about the random medium. In figure 4, we plot the values of the Arlequin estimates $\underline{K}^\varepsilon_N$ for three different correlation lengths ($\varepsilon = \ell_c/L = 10$, $\varepsilon = 1$, and $\varepsilon = 0.1$) as a function of the numbers of Monte Carlo trials N. As in the previous case, the Arlequin estimate depends on both the number of Monte Carlo trials, but also on those realizations themselves, so each value of $\underline{K}^\varepsilon_N$ is computed for $n = 10$ different ensembles of realizations of the random medium. On the same figure 4, we compare the Arlequin estimates with the KUBC and SUBC estimates discussed above.

The results are extremely convincing in the case presented here. Even when the correlation length is much smaller than the computational cell ($\varepsilon = 10$), the iterative Arlequin method predicts the correct homogenized coefficient, in the limit of large number of Monte Carlo realizations. The bias that is observed in the KUBC and SUBC estimates for large ε cancels completely for our estimate. However, it should be reminded that we have considered here the homogenization of a particular random medium. The random field $\boldsymbol{k}_\varepsilon$ is indeed locally invariant by inversion, and the homogenized tensor does not depend on the correlation structure. At this point, it therefore cannot be stated unambiguously whether the excellent behavior of our method is a coincidence or a general behavior. In any case, it should be stressed that the KUBC and SUBC approaches behave much worse than our Arlequin estimate. A first

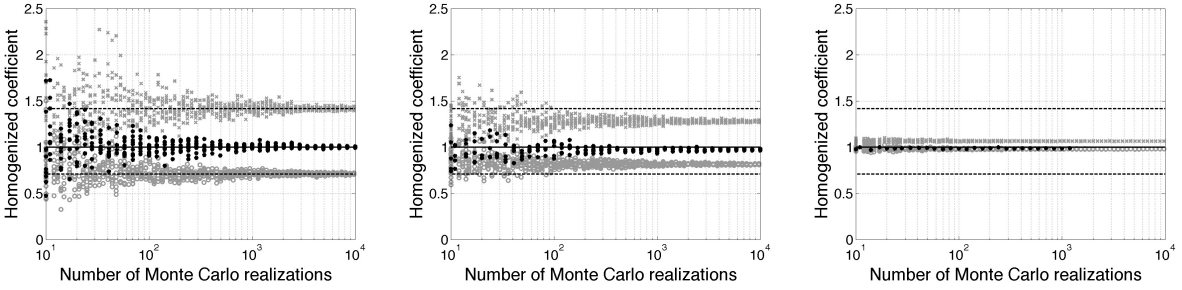

(a) $\varepsilon = 10$ (b) $\varepsilon = 1$ (c) $\varepsilon = 0.1$

Fig. 4. Convergence of the Dirichlet Arlequin estimate $\underline{\check{K}}_N^{\varepsilon}$ (black pluses) for different correlation lengths ((a) $\varepsilon = \ell_c/L = 10$, (b) $\varepsilon = 1$, and (c) $\varepsilon = 0.1$) as a function of the numbers of Monte Carlo trials N, and comparison with the KUBC $\check{K}_N^{\varepsilon}$ (light grey crosses) and SUBC $\hat{K}_N^{\varepsilon}$ (light grey circles) coefficients. The dashed lines indicate the values of the arithmetic average $\mathrm{E}[\boldsymbol{k}_\varepsilon]$ and of the harmonic average $\mathrm{E}[\boldsymbol{k}_\varepsilon^{-1}]^{-1}$. The solid lines indicate the value of $K^* = 1$.

explanation for this different behavior should be sought in the fact that we indeed have limited the influence of the boundary conditions by projecting them far away for the sample of interest.

5. Conclusions and prospects

In this paper, we have discussed a stochastic-deterministic coupling approach based on a very weak energy coupling operator. The introduction of this coupling approach allowed us to propose a new numerical scheme for the homogenization of random media. The results obtained for the chosen 2D example are spectacular. The bias observed in the KUBC and SUBC estimates completely vanishes, even for very large correlation length $\varepsilon = \ell_c/L$. This might put under question the widely-used concept of Representative Volume Element (RVE). Indeed, this RVE is usually understood as the (physical) size of the cell over which homogenization should be performed to yield the correct value of the homogenized coefficient. Our study would seem to show that this RVE vanishes in some cases. However, further studies are required to check the conditions under which this behavior is observed. Applications to polycrystals or matrix-inclusions materials, of interest for the composites and micro-mechanics communities, will be considered. Another approach will consist in deriving theoretical bounds linking the Arlequin estimates to both the theoretical homogenized coefficient and to the KUBC and SUBC estimates.

Acknowledgements

This work was partially supported by the ANR project TYCHE (Advanced methods using stochastic modeling in high dimension for uncertainty modeling, quantification and propagation in computational mechanics of solids and fluids), with project number ANR-2010-BLAN-0904, and by grants from DIGITEO and Région Ile-de-France, with project number 2009-26D.

References

[1] Ben Dhia H. Multiscale mechanical problems: the Arlequin method. Comptes Rendus de l'Académie des Sciences - Series IIB. 1998;326(12):899–904.

[2] Ben Dhia H, Rateau G. The Arlequin method as a flexible engineering design tool. International Journal for Numerical Methods in Engineering. 2005;62(11):1442–1462.

[3] Cottereau R, Ben Dhia H, Clouteau D. Localized modeling of uncertainty in the Arlequin framework. In: Belyaev A, Langley R, editors. IUTAM Symposium on the Vibration Analysis of Structures with uncertainties. IUTAM Bookseries. Springer; 2010. p. 477–488.

[4] Cottereau R, Clouteau D, Ben Dhia H, Zaccardi C. A stochastic-deterministic coupling method for continuum mechanics. Computer Methods in Applied Mechanics and Engineering. 2011;200(47-48):3280–3288.

[5] Zhikov VV, Kozlov SM, Oleinik OA, Ngoan KT. Averaging and G-convergence of differential operators. Russian Mathematical Surveys. 1979;34:69.

[6] Yurinskii VV. Averaging elliptic equations with random coefficients. Siberian Mathematical Journal. 1979;20(4):611–623.

[7] Kozlov SM. Averaging of random operators. Math USSR Sbornik. 1980;37(2):167–180.

[8] Papanicolaou GC, Varadhan SR. Boundary value problems with rapidly oscillating random coefficients. In: Fritz J, Lebowitz JL, editors. Proceedings of the Conference on Random Fields. vol. 2 of Seria Colloquia Mathematica Societatis Janos Bolyai. North Holland; 1981. p. 835–873.

[9] Sab K. On the homogenization and the simulation of random materials. European Journal of Mechanics A/Solids. 1992;11(5):585–607.

[10] Bourgeat A, Mikelić A, Wright S. Stochastic two-scale convergence in the mean and applications. Journal für die Reine und Angewandte Mathematik. 1994;1994(456):19–52.

[11] Bourgeat A, Kozlov SM, Mikelić A. Effective equations of two-phase flow in random media. Calculus of Variations and Partial Differential Equations. 1995;3(3):385–406.

[12] Lejay A. Homogenization of divergence-form operators with lower-order terms in random media. Probability Theory and Related Fields. 2001;120(2):255–276.

[13] Caffarelli LA, Souganidis PE, Wang L. Homogenization of fully nonlinear, uniformly elliptic and parabolic partial differential equations in stationary ergodic media. Communications in Pure and Applied Mathematics. 2005;58(3):319–361.

[14] Kanit T, Forest S, Galliet I, Mounoury V, Jeulin D. Determination of the size of the representative volume element for random composites: statistical and numerical approach. International Journal of Solids and Structures. 2003;40:3647–3679.

[15] Bourgeat A, Piatnitski A. Approximations of effective coefficients in stochastic homogenization. Annales de l'Institut Henri Poincaré. 2004;40:153–165.

[16] Héraud S, Allais L, Haddadi H, Marini B, Teodosiu C, Zaoui A. Du polycristal au multicristal: vers un mésoscope numérique. Journal de Physique IV. 1998;8(Pr4):27–32.

[17] Ben Dhia H, Rateau G. Mathematical analysis of the mixed Arlequin method. Comptes Rendus de l'Académie des Sciences - Series I - Mathématiques. 2001;332(7):649–654.

[18] Ben Dhia H. Further insights by theoretical investigations of the multiscale Arlequin method. International Journal for Multiscale Computational Engineering. 2008;6(3):215–232.

[19] Lagarias J, Reeds JA, Wright MH, Wright PE. Convergence properties of the Nelder-Mead simplex method in low dimensions. SIAM Journal for Optimization. 1998;9(1):112–147.

[20] Shinozuka M, Deodatis G. Simulation of stochastic processes by spectral representation. Applied Mechanics Reviews. 1991;44(4):191–205.

[21] Milton GW. The theory of composites. Cambridge Monographs on Applied and Computational Mechanics. Cambridge University Press; 2002.